A Study of Low Temperature and Low Stress Electroless Copper Plating Bath

Li-Sha Li, Xi-Rong Li, Wen-Xia Zhao, Qian Ma, Xu-Bin Lu, Zeng-Lin Wang[*]

Key Laboratory of Applied Surface and Colloid Chemistry (Shaanxi Normal University), Ministry of Education, School of Chemistry and Chemical Engineering, Xi'an, 710062, People's Rep. China
[*]E-mail: wangzl@snnu.edu.cn

To meet the requirement of PCB copper interconnection, a low temperature and low stress electroless copper plating bath containing Cu(II)-Rochell salt as complex was investigated. The effects of additives, such as 2,6-diaminopyridine as accelerator, 2,2'-dipyridyl as stabilizer, $NiSO_4 \cdot 6H_2O$ as stress-relief agent and sodium dodecyl sulfate as surfactant, on the deposition rate, deposited copper microstructure and surface morphology were investigated by deposition rate measurement and surface SEM observation. Though the deposition rate of electroless copper solution was accelerated by 2,6-diaminopyridine addition and was inhibited by 2,2'-dipyridyl addition, it reached 3.45 $\mu m \cdot h^{-1}$ at 33 °C with the composite addition of the four additives, and the deposited copper film also became smooth and uniform. The effects of additives on the polarization behaviors of the electroless copper plating bath were investigated by the linear sweep voltammetry method and mixed potential theory. The internal stresses of copper films were measured by XRD analysis method using the (220) and (311) peaks. The internal stresses of deposited copper film on the (220) and (311) crystal planes were decreased from -164.49 and -122.34 MPa to -16.50 and -31.00 MPa with an addition of 15.0 $mg \cdot L^{-1}$ $NiSO_4 \cdot 6H_2O$, and the adhesion strength between the substrate and electroless copper film was also increased from 0.84 to 1.12 $kN \cdot m^{-1}$. Finally, a low temperature and low stress electroless copper plating bath was obtained.

1. INTRODUCTION

Semi-additive process (SAP) is widely used to form metallic conductive patterns which are electroplated on the electroless deposited copper (Cu) seed layers on the surface of substrates [1]. Generally, the high adhesion strength between electroless copper film and substrate was obtained by surface etching process to enhance the surface roughness of the substrate. Recent advances are

required to have finer and thinner PCB substrates for the high integrated electronic devices [2]. With the further finer and thinner of the copper interconnection, a high surface roughness of the substrate leads to a dramatic attenuation for the high-frequency signal [3]. In order to assure the adhesive strength at the same time reduce the attenuation for the high-frequency signal, a low stress electroless copper plating bath became very essential.

Intrinsic stress of deposited copper film was influenced by the composition and the operation conditions of the electroless copper solution. Hsu and Chen reported that additive saccharin relieved the stress of electroless Ni-Cu-P deposit on Al foil [4, 5]. Kobayashi et al. demonstrated that the adhesion between epoxy resin and electroless copper was enhanced by an addition of sodium sulfide or triazine dithiole [6]. Seo and Bamberg reported that the strain of copper film could be weakened with an addition of nickel [7, 8]. However, there has no literature to report about low temperature and low stress electroless copper solution.

In order to obtain stable electroless copper solution, 2,2'-dipyridyl was usual used as the stabilizer to prevent spontaneous decomposition of the bath. However, the deposition rate of electroless copper solution decreased significantly with an addition of 2,2'-dipyridyl. Then the synergistic effects of accelerator 2,6-diaminopyridine with 2,2'-dipyridyl on the deposition rate and the stability of electroless copper solution were investigated. And the effects of surfactant SDS and $NiSO_4 \cdot 6H_2O$ on the surface morphology and stress of deposited Cu film were studied.

2. EXPERMENTAL PART

The ABS substrates with a thickness of 1.0 mm and an area of 40×25 mm were used in all experiments. First, the ABS substrates were pretreated by the degreasing and swelling processes [9]. Then the etching process, neutralizing process, sensitization process and activation process were carried according to our previous researches [10]. Distilled water was used to wash the substrates after every step.

The composition of electroless copper plating solution was $CuSO_4 \cdot 5H_2O$ (10.0 $g \cdot L^{-1}$) as a copper ion source, $NaKC_4H_4O_6 \cdot 4H_2O$ (28.25 $g \cdot L^{-1}$) as a complexing agent, HCHO (5 $mL \cdot L^{-1}$) as a reducing agent, 2,6-diaminopyridine as the accelerator, 2,2'-dipyridyl as the stabilizer, $NiSO_4 \cdot 6H_2O$ as the stress-relief agent and SDS as the surface activator. The pH of the plating bath was adjusted to 12.5 using NaOH solution, and the bath temperature was maintained at 33 °C.

The linear sweep voltammetry (LSV) was used to depict the effects of additives on the oxidation of HCHO and reduction of copper ions. The measurement method was carried according to literature [10]. The X-ray diffractometer (XRD) was used to measure and analyze the internal stress of the electroless copper films [11, 12]. A Cu target with a wave length of 0.1506 nm was used as the X-ray radiator. The particular (h k l) planes of deposited copper films were scanned at 4 $°\cdot min^{-1}$ and the degree increment were 0.1 °. The working voltage and current were 40 kV and 40 mA, respectively. The $2\theta_\psi$-$\sin^2\psi$ method was applied for the internal stress evaluation [13] and the diffracted peaks (220) and (311) were selected to determine the internal stresses of the deposited copper film.

The adhesion strength between film and substrate was measured using a 90 ° peel test at a peel rate of 25 mm·min^{-1} [14]. The microstructure and surface morphology of samples were characterized by scanning electron microscope (SEM).

3. RESULTS AND DISCUSSION

3.1 Synergistic effect of additives on the deposition rate and surface morphology of deposited copper films

The electroless copper bath is usual easy to be decomposed without a stabilizer addition, but the addition of the stabilizer would lead to a significant decrease of the deposition rate. In order to improve the stability of electroless copper solution at the same time maintain a high deposition rate at low bath temperature, a accelerator should not only accelerate electroless copper deposition, but also have a better synergistic effect with stabilizer to inhibit a significant decrease of the deposition rate. And so, the synergy effects of some accelerators such as 8-hydroxy-7-iodo-5-quinoline sulfonic acid, 2-mercaptobenzothiazole, 2,6-diaminopyridine, triethanolamine, and bis-3-sulfopropyl-disulfide and inhibitors such as 2,2'-dipyridyl, $K_4[Fe(CN)_4]$ on the deposition rate were first investigated [10, 15-19]. And the better synergy effect only between 2,6-diaminopyridine and 2,2'-dipyridyl on the deposition rate of electroless copper solution was obtained.

As shown in Fig.1, the deposition reaction in the electrolyte was inhibited by an addition of 2,2'-dipyridyl, but was accelerated by an addition of 2,6-diaminopyridine.
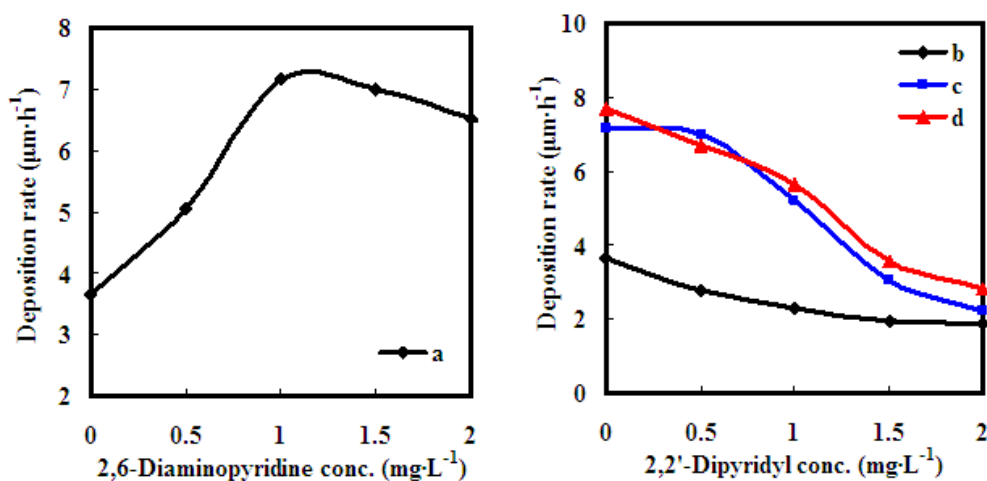

Figure 1. Effects of additives on the deposition rate of the electroless copper plating solution. (a) 2,6-diaminopyridine; (b) 2,2'-dipyridyl; (c) 2,2'-dipyridyl with 1.0 mg·L^{-1} 2,6-diaminopyridine; (d) 2,2'-dipyridyl with 1.0 mg·L^{-1} 2,6-diaminopyridine and 15.0 mg·L^{-1} $NiSO_4·6H_2O$.

The deposition rate of electroless copper solution was increased from 3.65 to 7.16 μm·h^{-1} with alone addition 1.0 mg·L^{-1} 2,6-diaminopyridine (Fig.1a), and it was decreased from 3.65 to 1.95 μm·h^{-1}

with alone addition 1.5 mg·L^{-1} 2,2'-dipyridyl (Fig.1b). However, when 2,6-diaminopyridine concentration was 1.0 mg·L^{-1}, the deposition rate of electroless copper solution decreased from 7.16 to 3.03 μm·h^{-1} with an addition of 1.5 mg·L^{-1} 2,2'-dipyridyl (Fig.1c), which indicated a better synergistic effect between 2,6-diaminopyridine and 2,2'-dipyridyl on inhibiting the significant decrease of the deposition rate caused by alone addition 2,2'-dipyridyl. Not only the deposition rate of electroless copper solution was increased to some extent, but also the stability of the electroless copper solution and the surface morphology of the deposited copper films were improved with the two additives addition.

To decrease deposited copper film stress, $NiSO_4 \cdot 6H_2O$ as stress-relieving agent was added to the electroless copper solution. And it was found that the deposition rate of electroless copper solution increased slightly with an alone addition of $NiSO_4 \cdot 6H_2O$ or combing with 2,6-diaminopyridine and 2,2'-dipyridyl (Fig.1d).
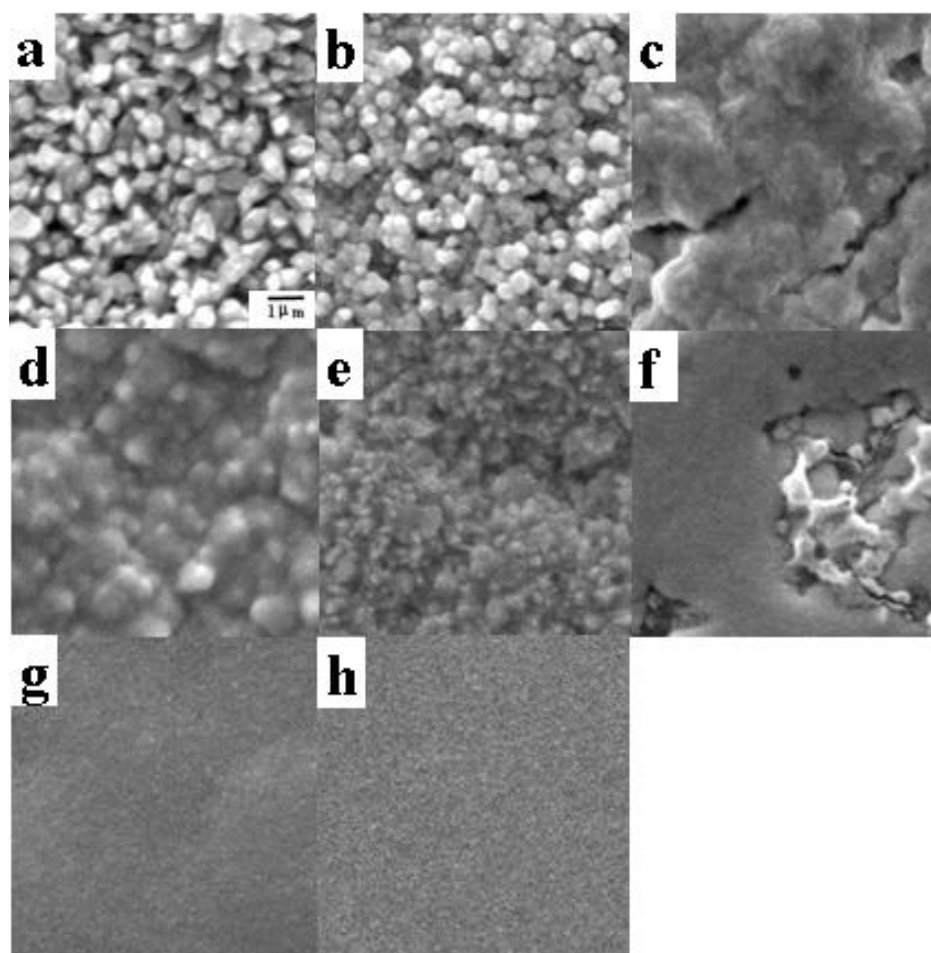

Figure 2. SEM images of deposited copper films in the baths with different additives: (a) additive-free; (b) 1.0 mg·L^{-1} 2,6-diaminopyridine; (c) 1.5 mg·L^{-1} 2,2'-dipyridyl; (d) 15.0 mg·L^{-1} $NiSO_4 \cdot 6H_2O$; (e) 4.0 mg·L^{-1} SDS; (f) 1.0 mg·L^{-1} 2,6-diaminopyridine and 1.5 mg·L^{-1} 2,2'-dipyridyl; (g) 1.0 mg·L^{-1} 2,6-diaminopyridine, 1.5 mg·L^{-1} 2,2'-dipyridyl and 15.0 mg·L^{-1} $NiSO_4 \cdot 6H_2O$; (h) 1.0 mg·L^{-1} 2,6-diaminopyridine, 1.5 mg·L^{-1} 2,2'-dipyridyl, 15.0 mg·L^{-1} $NiSO_4 \cdot 6H_2O$ and 4.0 mg·L^{-1} SDS.

Hydrogen gas trapped in the deposit is a major cause of blister formation, which evolves inevitably during electroless Cu deposition. SDS as surfactant was used to decrease the surface tension of the electroless copper solution and eliminate hydrogen bubbles formed on the surface of electroless Cu film by the reducing agent dehydrogenation reaction [20]. Furthermore, the deposition rate of electroless copper solution did not change apparently no matter if the SDS was added alone or combining with other additives.

Fig.2 represented the surface morphology of the deposited copper films obtained at different composition of additives. The surface morphology of the deposited copper film in the basic bath exhibited rough (see Fig.2a). With an alone addition of the additives, the surface morphology of the deposited copper films were same as that in the basic bath (see Fig.2b-2e), which indicated that the surface morphology of the copper films could not be improved by an alone addition of the additives. However, when 1.0 mg·L^{-1} 2,6-diaminopyridine and 1.5 mg·L^{-1} 2,2'-dipyridyl were added to the electroless copper solution, the surface morphology of deposited copper film was ameliorated to some extent (see Fig.2f). Further, when 1.0 mg·L^{-1} 2,6-diaminopyridine, 1.5 mg·L^{-1} 2,2'-dipyridyl and 15.0 mg·L^{-1} NiSO$_4$·6H$_2$O were added to the electroless copper solution, the surface morphology became smooth and uniform (see Fig.2g). The results indicated that the surface morphology of the copper had not been improved with an addition of any additive alone, but the combination of the above three additives with their optimized concentrations was very conducive to refine the crystalline size and improve the surface morphology of the deposited copper film. When SDS was added to the electroless copper solution combing with the three additives, the topography of the deposited copper film was very smooth and uniform (see Fig.2h). And, the color of the Cu film was changed from dark red to copper-bright color.

3.2 Effects of additives on the oxidation of HCHO and reduction of copper ions.

According to the mixed potential theory, the overall reaction of the electroless process was separated into the reduction of copper ions and the oxidation of the reducing agent, and the deposition rate was determined by the two half-reactions on the same electrode. And so, the LSV measurement is useful to understand the effects of additives on the half-reactions in the electrolyte [21, 22]. Fig.3 and Fig.4 showed the LSV for HCHO oxidation and copper ions reduction on the copper electrode in an electrolyte. It was found that the HCHO oxidation peaks occurred at more negative potentials than the copper ions reduction peaks, so the overall reaction of the electroless copper plating process was controlled by current densities of the oxidation and reduction.

The polarization curves of the HCHO oxidation and copper ions reduction reaction in the basic bath were shown in Fig.3A(a) and Fig.3B(a). With an addition of 1.0 mg·L^{-1} 2,6-diaminopyridine, the HCHO oxidation peak current and the copper ions reduction peak current were increased from 0.44 and 0.53 mA·cm^{-2} to 0.52 and 0.67 mA·cm^{-2} (see Fig.3A(b) and Fig.3B(b)), which indicated that 2,6-diaminopyridine not only accelerated the HCHO oxidation, but also accelerated the copper ions reduction. When 1.5 mg L^{-1} 2,2'-dipyridyl was added to the basic bath, the oxidation peak current and the reduction peak current decreased from 0.44 and 0.53 mA·cm^{-2} to 0.38 and 0.47 mA·cm^{-2} (see

Fig.3A(c) and Fig.3B(c)). With an addition of 15.0 mg·L⁻¹ NiSO₄·6H₂O, the HCHO oxidation peak shifted from -0.380 to -0.414 V (see Fig.3A(d)), which indicated that reduction capacity of HCHO in the electrolyte could be enhanced by the presence of nickel ions [19, 22]. However, the oxidation peak current and the reduction peak current changed a little with an addition of NiSO₄·6H₂O, which was in agreement with the deposition rate measurement.
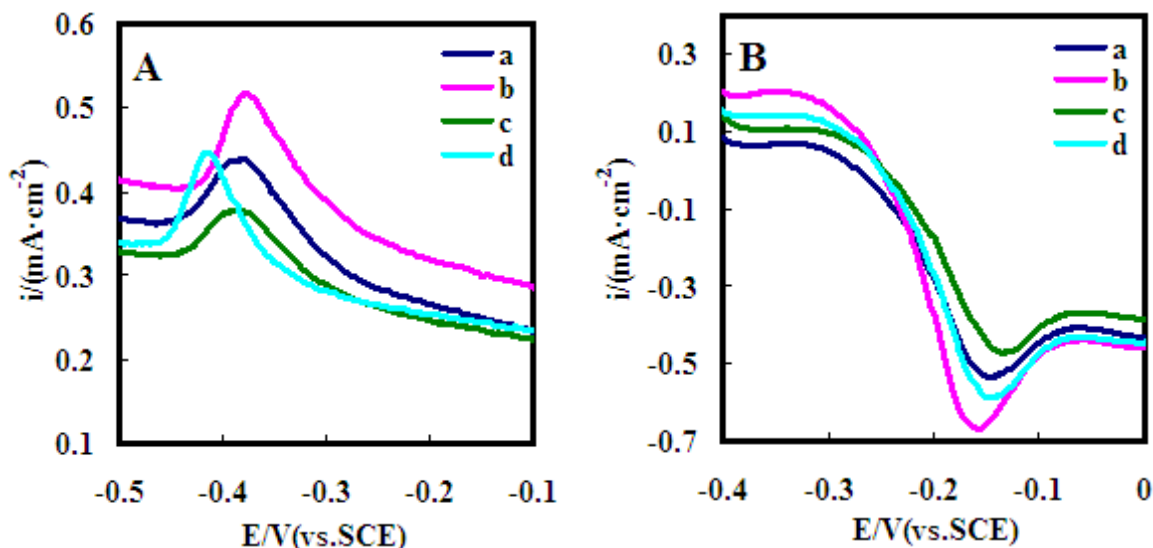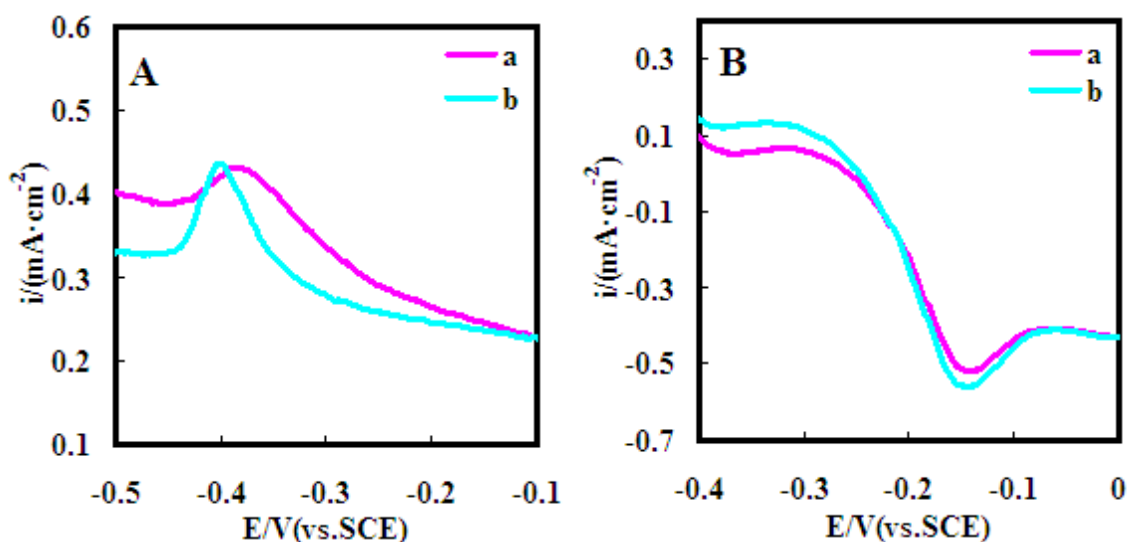

Figure 3. The effects of additives on the (A) HCHO oxidation polarization, and (B) copper ions reduction polarization behaviors of electroless copper plating solution. (a) additive-free; (b) 1.0 mg·L⁻¹ 2,6-diaminopyridine; (c) 1.5 mg·L⁻¹ 2,2'-dipyridyl; (d) 15.0 mg·L⁻¹ NiSO₄·6H₂O.

Figure 4. The effects of additives on the (A) HCHO oxidation polarization, and (B) copper ions reduction polarization behaviors of electroless copper plating solution: (a) 1.0 mg·L⁻¹ 2,6-diaminopyridine and 1.5 mg·L⁻¹ 2,2'-dipyridyl; (b) 1.0 mg·L⁻¹ 2,6-diaminopyridine, 1.5 mg·L⁻¹ 2,2'-dipyridyl and 15.0 mg·L⁻¹ NiSO₄·6H₂O.

When 2,2'-dipyridyl and 2,6-diaminopyridine concentrations were 1.5 mg·L⁻¹ and 1.0 mg·L⁻¹ in the electrolyte, the HCHO oxidation peak current and the copper ions reduction peak current were

increased to 0.43 and 0.52 mA·cm^{-2} (see Fig.4A(a) and Fig.4B(a)), which was higher than that with an alone addition of 2,2'-dipyridyl (0.38 and 0.47 mA·cm^{-2}), and was in agreement with the deposition rate measurement. Further, when 15.0 mg·L^{-1} NiSO$_4$·6H$_2$O was added to the above mentioned solution, though the oxidation peak potential was migrated from -0.386 V to -0.400 V, the oxidation peak current and the reduction peak current increased a little (see Fig.4A(b) and Fig.4B(b)), which was consistent with the deposition rate change with the additives.

3.3 Internal stress and adhesion strength measurements of deposited copper film

Internal stresses of the copper films were analyzed using XRD by a $2\theta_\psi$-$\sin^2\psi$ method which was based on the measurement of the shift of a diffraction peak position recorded for different tilt angles ψ, and the angles ψ ranged from 0 ° to 40 ° [13]. The diffraction angle $2\theta_\psi$ on a particular (h k l) plane was measured as a function of ψ, and the internal stress σ could be calculated from the slope of the $2\theta_\psi$-$\sin^2\psi$ curve through the formula as follow:

$$\sigma = -\frac{E}{2(1+v)} ctg\theta \frac{\pi}{180} \frac{\partial 2\theta_\psi}{\partial \sin^2\psi} \qquad (1)$$

Here, θ was the diffraction angle of stress-free Cu film, and E (119×10^3 MPa) and v (0.34) were the Young modulus and Poisson ratio of the Cu film, respectively [23]. Diffraction peaks of different (h k l) planes were decreased with angle ψ due to absorption by the copper films [11]. The higher the diffraction angle 2θ, the more accurate the measurement was [24, 25]. And so, the Cu (220) and Cu (311) crystal planes were chosen to evaluate the internal stresses, whereas the Cu (222) peak was too weak to be used to evaluate stress measurements.
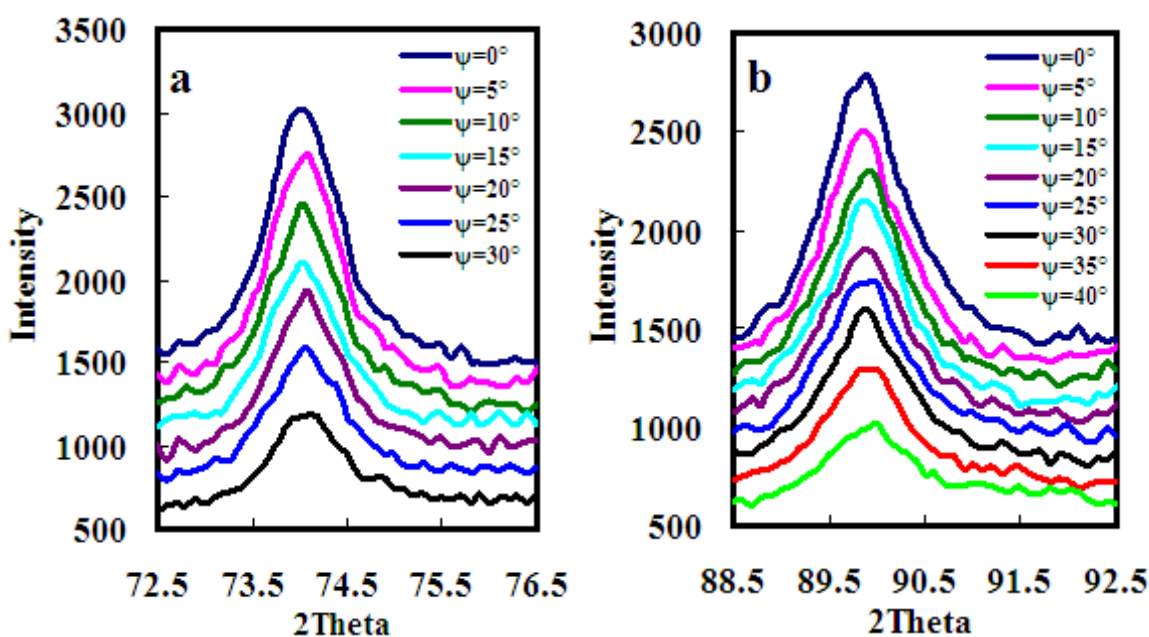

Figure 5. XRD patterns of the electroless copper film with angles ψ on the (a) (220) plane, and (b) (311) plane without NiSO$_4$·6H$_2$O in the electrolyte.

Then when 2,6-diaminopyridine, 2,2'-dipyridyl and SDS concentration were 1.0 mg·L^{-1}, 1.5 mg·L^{-1}, and 4.0 mg·L^{-1}, the effect of NiSO$_4$·6H$_2$O concentration (0, 5.0, 10.0, 15.0 and 20.0 mg·L^{-1}) on internal stress of the Cu film was investigated. Fig.5 showed the copper film diffraction peaks of (220) and (311) planes with different angles ψ without NiSO$_4$·6H$_2$O in the electrolyte. Fig.6 showed the (220) and (311) diffraction peaks with different angles ψ when NiSO$_4$·6H$_2$O concentration was 15.0 mg·L^{-1} in the electrolyte.
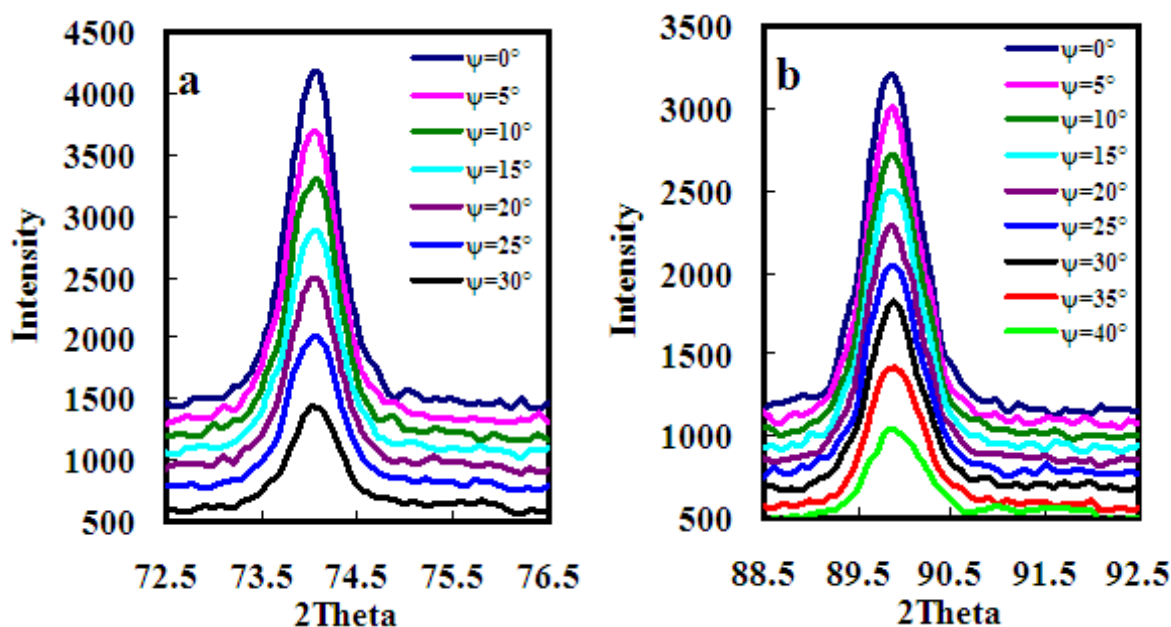

Figure 6. XRD patterns of the electroless copper film with the angles ψ on the (a) (220) plane, and (b) (311) plane when NiSO$_4$·6H$_2$O concentration in the electrolyte was 15.0 mg·L^{-1}.

From Fig.5 and Fig.6, it was found that the diffraction angles of (220) and (311) planes were shifted with an increase of ψ angle, and the diffraction intensities of (220) and (311) planes decreased with an increase of ψ angle. On the other hand, it was found that the diffraction intensities strengthened significantly with the addition of NiSO$_4$·6H$_2$O, which indicated that NiSO$_4$·6H$_2$O enhanced the crystallinity of deposited copper film. Taking $2\theta_\psi$-$\sin^2\psi$ as ordinate and abscissa axis, the linear relationship between $2\theta_\psi$ and $\sin^2\psi$ on the (220) and (311) planes with the NiSO$_4$·6H$_2$O concentrations were shown in Fig.7 and Fig.8. Then the slopes of $2\theta_\psi$-$\sin^2\psi$ straight line with the NiSO$_4$·6H$_2$O concentrations were obtained by the least square approximation, and the results were listed in Table 1. After putting the slope values of $2\theta_\psi$-$\sin^2\psi$ into equation (1), the internal stress values of deposited Cu films versus the NiSO$_4$·6H$_2$O concentration in the electrolyte were obtained, and the results were listed in Table 2.

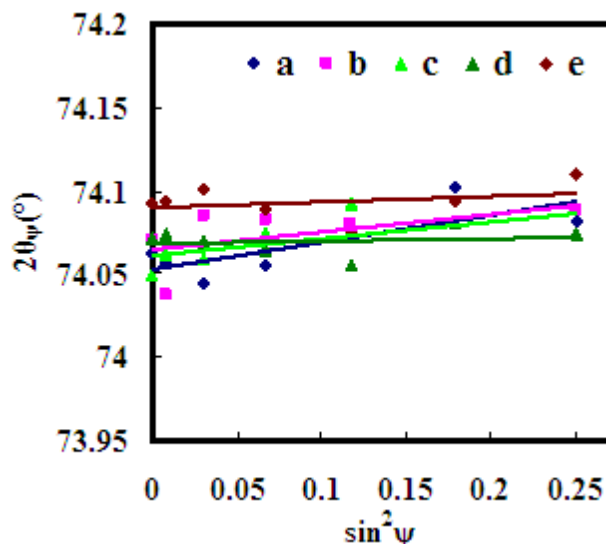**Figure 7.** The $2\theta_\psi$-$\sin^2\psi$ curves of the deposited copper film on the (220) plane with $NiSO_4 \cdot 6H_2O$ conc.: (a) 0; (b) 5.0; (c) 10.0; (d) 15.0; (e) 20.0 mg·L^{-1}.

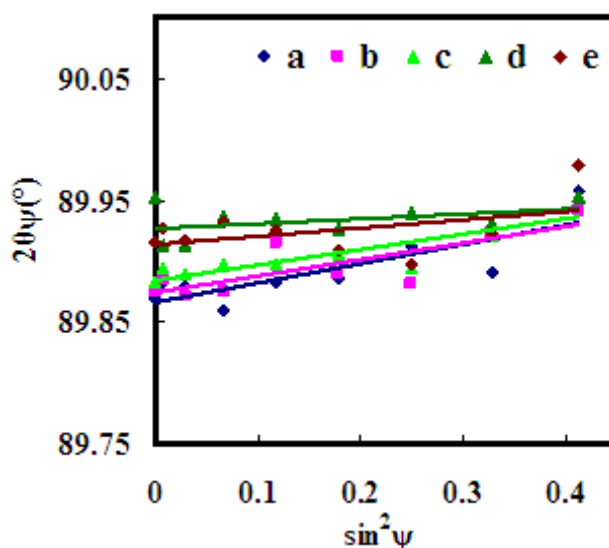**Figure 8.** The $2\theta_\psi$-$\sin^2\psi$ lines of the deposited copper film on the (311) plane with $NiSO_4 \cdot 6H_2O$ conc.: (a) 0 ; (b) 5.0; (c) 10.0; (d) 15.0; (e) 20.0 mg·L^{-1}.

Table 1. The slopes of the $2\theta_\psi$-$\sin^2\psi$ lines for deposited copper films on the (220) and (311) planes with the $NiSO_4 \cdot 6H_2O$ concentration.

$NiSO_4 \cdot 6H_2O$ conc. (mg·L^{-1})	0.0	5.0	10.0	15.0	20.0
the slope on the (220) plane	0.16	0.10	0.10	0.02	0.03
the slope on the (311) plane	0.16	0.14	0.13	0.04	0.07

From the Table 2, it was found that the internal stress value of the deposited copper films for the (220) plane was -164.49 MPa without $NiSO_4 \cdot 6H_2O$ in the electrolyte, and it was decreased with an addition and the increasing concentration of $NiSO_4 \cdot 6H_2O$. When $NiSO_4 \cdot 6H_2O$ concentration in the electrolyte was 15.0 mg·L^{-1}, the internal stress value reached the minimum value -16.50 MPa. For the (311) plane, the change trend of the internal stress value with an addition and increasing concentration of $NiSO_4 \cdot 6H_2O$ was same as for the (220) plane, and the internal stress of the copper films decreased from -122.3 to -31.0 MPa with $NiSO_4 \cdot 6H_2O$ concentration from 0 to 15.0 mg·L^{-1}. The result indicated that the internal stress of electroless copper film could be relieved with an addition of $NiSO_4 \cdot 6H_2O$ in the electrolyte.

Table 2. The internal stresses of deposited copper films on the (220) and (311) planes with the $NiSO_4 \cdot 6H_2O$ concentrations.

$NiSO_4 \cdot 6H_2O$ conc. (mg·L^{-1})	0.0	5.0	10.0	15.0	20.0
the stress on the (220) plane (MPa)	-164.49	-106.09	-105.34	-16.50	-34.29
the stress on the (311) plane (MPa)	-122.34	-105.61	-97.19	-31.00	-51.56

The initial islands of the growing Cu film were compressed upon deposition in the copper deposition process and these individual islands coalesced into larger islands with the elapse of deposition time [26-28]. And the intrinsic stress was created by the coalescence of neighboring islands which was caused by the flow of atoms between the grain boundaries of the film and the substrate surface within nodules [29, 30]. As shown in Fig.2, the copper particles formed from the bath with the addition of $NiSO_4 \cdot 6H_2O$ were finer than that from the bath without nickel, and did not coalesce without the prominent nodule structure in the progress of the electroless copper plating, which indicated that the addition of $NiSO_4 \cdot 6H_2O$ increased the number of the nodules and restrained coalescence of the islands within nodules by disrupting the transport of the Cu atoms during electroless deposition [31, 32]. Consequently, the energy of stress was released significantly by the addition of $NiSO_4 \cdot 6H_2O$ with the formation of nodule boundaries and a lower stress was obtained. However, the internal stress increased slightly when $NiSO_4 \cdot 6H_2O$ concentration was 20.0 mg·L^{-1}, which was attributed to that the neighboring Ni atoms might also coalesce during deposition.

Table 3. The adhesion strengths between ABS substrates and the deposited copper films with the $NiSO_4 \cdot 6H_2O$ concentration.

$NiSO_4 \cdot 6H_2O$ conc. (mg·L^{-1})	0	5.0	10.0	15.0	20.0
the adhesion strength (kN·m^{-1})	0.84	0.92	0.94	1.12	1.06

Though the adhesion between the copper film and the substrate was partially attributed to mechanical anchoring effect, it could be influenced by the internal stress of the Cu film [6]. In order to verify the change trend of the internal stress value with the concentration of $NiSO_4 \cdot 6H_2O$ in the electrolyte, the adhesion strengths between ABS substrates and electroless copper film deposited in the electrolyte with different $NiSO_4 \cdot 6H_2O$ concentrations were measured, and the results were shown in Table 3. It was found that the adhesion strength between the substrate and electroless copper film without $NiSO_4 \cdot 6H_2O$ was 0.84 $kN \cdot m^{-1}$. It was increased with the addition and the increasing of the $NiSO_4 \cdot 6H_2O$ concentration, and reached the maximum value 1.12 $kN \cdot m^{-1}$ when $NiSO_4 \cdot 6H_2O$ concentration in the electrolyte was 15.0 $mg \cdot L^{-1}$. The results were in agreement with the internal stress measurement of deposited copper film and indicated that low stress electroless copper plating bath was obtained by the composite addition of $NiSO_4 \cdot 6H_2O$ and other additives, and the stress measurement using XRD by a $2\theta_\psi$-$\sin^2\psi$ method was very effective.

4. CONCLUSION

A low temperature and low stress electroless copper plating bath containing Cu(II)-Rochell salt as complex was investigated. The deposition rate of electroless copper solution was accelerated by 2,6-diaminopyridine and was inhibited by 2,2'-dipyridyl. When 1.0 $mg \cdot L^{-1}$ 2,6-diaminopyridine, 1.5 $mg \cdot L^{-1}$ 2,2'-dipyridyl, 15.0 $mg \cdot L^{-1}$ $NiSO_4 \cdot 6H_2O$ and 4.0 $mg \cdot L^{-1}$ SDS were added to the bath, the deposition rate reached 3.45 $\mu m \cdot h^{-1}$, and the deposited copper film became smooth and uniform. The effects of additives on the polarization behaviors of the electroless copper plating bath were investigated by the linear sweep voltammetry method and mixed potential theory. The internal stresses of the copper films were measured by XRD analysis method using the (220) and (311) peaks. The internal stresses of deposited copper film on the (220) and (311) crystal planes were decreased from -164.49 and -122.34 MPa to -16.50 and -31.00 MPa with an addition of 15.0 $mg \cdot L^{-1}$ $NiSO_4 \cdot 6H_2O$, and the adhesion strength between the substrate and electroless copper film was also increased from 0.84 to 1.12 $kN \cdot m^{-1}$. In conclusion, a low temperature and low stress electroless copper plating bath was obtained.

References

1. R. Huemoeller, S. Rusli, S. Chiang, T. Y. Chen, D. Baron, L. Brandt and B. Roelfs, *Adv. Microelectron.*, 34 (2007) 22
2. G. Dehm, T. J. Balk, H. Edongué and E. Arzt, *Microelectron. Eng.*, 70 (2003) 412-424
3. P. Hutapea, J. L. Grenestedt, *Microelectron. Int.*, 24(1) (2007) 15-22
4. J. C. Hsu, K. L. Lin, *Thin Solid Films*, 471 (2005) 186-193

5. C. J. Chen, K. L. Lin, *Thin Solid Films*, 370 (2000) 106-113
6. T. Kobayashi, I. Mochizuki, H. Takahashi and H. Honma, *J. Surf. Finish. Soc. Jpn.*, 50(1) (1999) 101-102
7. J. W. Seo, H. S. Nam, S. Lee and Y. S. Won, *Korean J. Chem. Eng.*, 29(4) (2012) 529-533
8. S. Bamberg, L. K. Perry, B. Muir, A. Abuzir, F. Brüning and R. Brüning, *Thin Solid Films*, 520 (2012) 6935-6941
9. Z. X. Li, N. Li, L. Yin, Y. He and Z. L. Wang, *J. Electrochem. Soc.*, 12(12) (2009) D92-D95
10. X. Wang, N. Li, Z. F. Yang and Z. L. Wang, *J. Electrochem. Soc.*, 157(9) (2010) D500-D502
11. R. Brüning, B. Muir, E. McCalla, É. Lempereur, F. Brüning and J. Etzkorn, *Thin Solid Films*, 519 (2011) 4377-4383
12. M. Gelfi, E. Bontempi, R. Roberti and L. E. Depero, *Acta Mater.*, 52 (2004) 583-589
13. M. Yu, J. Z. Zhang, D. X. Li, Q. L. Meng and W. Z. Li, *Surf. Coat. Tech.*, 201 (2006) 1243-1249
14. Z. L. Wang, O. Yaegashi, H. Sakaue, T. Takahagi and S. Shingubara, *J. Appl. Phys.*, 7 (2003) 4697-4701
15. L. N. Schoenber, *J. Electrochem. Soc.*, 119 (11) (1972) 1491-1493
16. F. Hanna, Z. A. Hamid, A. A. Aal, *Mater. Lett.*, 58 (2003) 104-109
17. C. J. Dubois, A. E. Elia, J. C. Figueroa, *US patent 2012/0234682 A1*, (2012)
18. C. H. Lee, S. C. Lee, J. J. Kim, *Electrochim. Acta*, 50 (2005) 3563-3568
19. J. Li, H. Hayden and P. A. Kohl, *Electrochim. Acta*, 49 (2004) 1789-1795
20. N. Nwosu, A. Davidson, C. Hindle and M. Barker, *Ind. Eng. Chem. Res.*, 51 (2012) 5635-5644
21. J. Li, P. A. Kohl, *J. Electrochem. Soc.*, 149(12) (2002) C631-C636
22. X. P. Gan , K. C. Zhou, W. B. Hu and D. Zhang, *Surf. Coat. Tech.*, 206 (2012) 3405-3409
23. P. Dixit, Y. F. Sun, J. M. Miao, J. H. L. Pang, R. Chatterjee and R. R. Tummala, *J. Electrochem. Soc.*, 155(12) (2008) H981-H986
24. X. J. Zheng, J. Y. Li and Y. C. Zhou, *Acta Mater.*, 52 (2004) 3313-3322
25. C. H. Ma, J. H. Huang and H. Chen, *Thin Solid Films*, 418 (2002) 73-78
26. N. Fukumuro, M. Yamazaki, K. Ito, H. Ishihara, S. Kakunai, S. Yae and H. Matsuda, *J. Electrochem. Soc.*, 10(6) (2007) E14-E15
27. R. C. Cammarata, T. M. Trimble, *J. Mater. Res.*, 15(11) (2000) 2468-2474
28. B. W. Sheldon, K. H. A. Lau and A. Rajamani, *J. Appl. Phys.*, 90(10) (2001) 5097-5103
29. A. L. D. Vecchio, F. Spaepen, *J. Appl. Phys.*, 101(6) (2007) 063518 (1-9)
30. Z. Chen, X. D. Xu, C. C. Wong and S. Mhaisalkar, *Surf. Coat. Tech.*, 167 (2003) 170-176
31. D. Chocyk, T. Zientarski, A. Proszynski, T. Pienkos, L. Gladyszewski and G. Gladyszewski, *Cryst. Res. Technol.*, 40(4/5) (2005) 509-516
32. J. C. Hsu, K. L. Lin, *J. Mater. Res.*, 18(9) (2003) 2221-2227